Available online at www.sciencedirect.com

ScienceDirect

Procedia Engineering 81 (2014) 1842 – 1847

Procedia Engineering

www.elsevier.com/locate/procedia

11th International Conference on Technology of Plasticity, ICTP 2014, 19-24 October 2014, Nagoya Congress Center, Nagoya, Japan

Effects of contact pressure, plastic strain and sliding velocity on sticking in cold forging of aluminium billet

Laurent Dubar*, Catalin I. Pruncu, André Dubois, Mirentxu Dubar

TEMPO Lab., University of Valenciennes, F-59313 Valenciennes Cedex 9, France

Abstract

Hot rolling of stainless steel is one of the most important steps in manufacturing process regarding surface quality of the product. Stabilised ferritic stainless steels are widely used in automotive and cosmetic appliances but are also concerned by sticking phenomenon. These grades, having high dry corrosion and creep resistance, are enriched in specific chemical elements such as Cr, Nb or Ti, limiting also slab oxidation during hot rolling. Nevertheless, the mastered oxidation of slab surface is a way to protect metal surface from direct contact with rolls. In order to better understand initiation of sticking, a first campaign was based on topography and rolls surface state wear analysis. This study revealed that sticking initiation is not due to the presence of roll scratches which depth is higher than oxide layer thickness. Indeed, the probability that roll scratches are deeper than oxide layer thickness is very low. In a second time, a pilot was designed, reproducing tribological conditions of a roll bite, to better understand mechanisms that initiate sticking. Keeping in mind the importance of rolls and slab surface state, this pilot is able to use specimen taking from industrial products, having the original oxide layer surface. This second study highlighted the major role of silicon oxides on scale adherence and the high heterogeneity of this scale layer in thickness and in chemical composition.

Selection and peer-review under responsibility of the Department of Materials Science and Engineering, Nagoya University

Keywords: Aluminium alloys; Metal forming; Surface defects

* Corresponding author. Tel.: +33-327-511-380.
E-mail address: laurent.dubar@univ-valenciennes.fr

Selection and peer-review under responsibility of the Department of Materials Science and Engineering, Nagoya University
doi:10.1016/j.proeng.2014.10.243

1. Introduction

The high performance in terms of strength, together with lightweight, long lifespan and easy recycling, suggest aluminium alloys to be exploited on branch like transport industry [1,2]. While most of aluminium parts for the aerospace industry are machined, shipbuilding components for naval branch [3] or automotive chassis parts [4] are developed by forging.

In the cold forming process, an important aspect is related to the influence of equivalent plastic strain of the surface interaction (tool and specimen surface) [5]. Hence, the high rate of variation of plastic deformation, normal pressure, sliding speed, temperature, lubricant distribution and rheological behaviour, together with the progress of sticking cause the wear of the tool surface. Researchers spent quite a lot of time in comparing FEM simulations and laboratory/industrial experiments. Therefore, "local" [6] or "global" [7] models proposed were derived from standard [8] or/and modified [9] Archard's law [10]. The Archard's model requires the identification of a dimensionless wear constant K, which depends on temperature, thickness of lubricant layer, material transfer size, etc. This may be time consuming and requires expensive devices to evaluate the forming process. To overcome these difficulties, an innovative approach to quantify the risk of tool damage occurrence is initiated in the present study. For that purpose, wear and surface defects will be predicted by an expert system called Tool Surface Degradation in metal forming-expert system, which will make a link between results of finite element analyses and a specific database: the Library of Damage Indicators.

The present work presents the functioning of the expert system and the central part of the L.D.I. It deals with the feasibility of the new approach by presenting results from a simple cold forming operation. The results mainly focus on the forming of Al6082 aluminium alloy because of its well-known tendency to cause adhesive wear on forming and cutting tools. The effect of lubricant (MoS_2) is considered in the present paper.

2. Experimental Procedures

2.1. As received materials

Twenty-four samples of aluminium alloy Al6082 with 2.0 mm thickness were considered in this survey. Quasi-static tension tests, with a crosshead speed displacement of 0.5 mm/s, were performed to detect the mechanical properties in the rolling direction (RD). Thus, the mean values of these properties are: Yield Stress 296 MPa, Tensile Strength 330MPa and Fracture strain 26%. Chemical compositions of this material are presented in Semari et al. [11].

2.2. Experiments carried out on the analysed material

Tribological tests were performed on the Upsetting Sliding Test device (UST), developed in the authors' laboratory. This tribological test allows to perform friction test with contact pressures, plastic strains and sliding velocities closed to the ones encountered in cold forming processes. During the test, a contactor made of tool steel comes in contact with the specimen, slightly penetrates it, and slides against its surface where it creates a plastic strain (see Fig. 1a). UST adjustment parameters are the shape of the contactor, its penetration depth into the specimen and its sliding velocity. The experimental methodology and the relation between adjustment parameters and contact pressure and plastic strain are described in details in Ref. [12]. UST results are friction stresses, the evolution of surface roughness and the nature of the material transfer from one body to the other [13]. Identification of friction stresses for a large set of contact pressures lead to the identification of friction coefficients (Coulomb's, Tresca's or a generalised nonlinear models).

The dimensions of the specimens tested in this study are: L=40 mm, l=10 mm, and h=2 mm. The geometry of the contactors is a cylinder with a 20 mm radius. Upsetting sliding tests were performed at room temperature with respect to the following conditions:

- imposed penetration depth, Δh: 0.04, 0.07, 0.095, 0.12, 0.18 mm;
- sliding velocity, V_S: 10mm/s;
- true sliding distance: 40 mm;
- mean arithmetic surface roughness of the contactors: Ra ≈ 0.3 µm;
- lubrication conditions: dry test and MoS_2 (thickness of solid lubricant layer about 10 µm);

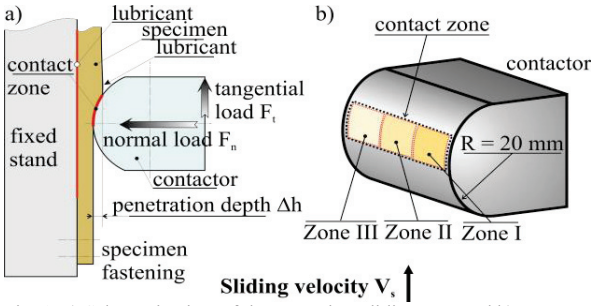

Fig. 1. a) Schematic view of the Upsetting-sliding test, and b) Zones of analysis considered for the contactor surface.

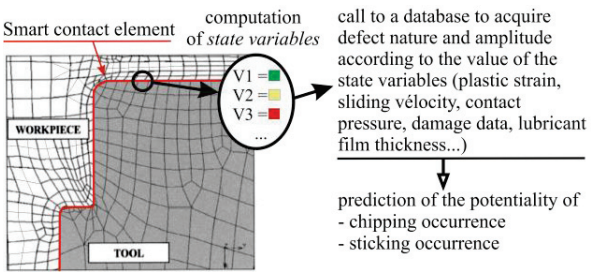

Fig 2. Illustration of the Tool Surface Degradation in metal forming Expert System.

2.3. Examined surfaces

Contactor and specimen surfaces that are in direct contact were analysed with 3D optical profilometer and Scanning Electron Microscopy (SEM) in order to achieve a better understanding of tribological phenomena.

The total area of the contactor that went into contact during the UST is between 11 and 30 mm², depending on penetration depth value Δh. Since the overall contact area was not possible to be assessed with the profilometry device in one unique measurement, the contact region was divided in three distinct zones. A schematic view of the contactor with specified reference zones is presented in Figure 1b. This approach also allowed to evaluate precisely the amount of material deposited on the contactor surface in the transverse direction.

UST are performed so that the sliding direction correspond to the longitudinal direction “L” of the specimens. It can be noticed that all surfaces have an initial roughness value Ra around 0.3 µm, with uniform level of roughness asperities in any region of the inspected surfaces.

In order to reduce friction and avoid direct contact between contactor and specimen sample, specimens were lubricated with molybdenum disulphide (MoS2) solid lubricant. Two tests without lubricant were performed to compare them with the lubricated ones.

3. Computation of Tool Surface Degradation: a new Expert System

The Tool Surface Degradation expert system intends to make a connection between results from the smart contact elements (i.e. numerical simulation) and the Library of Damage Indicators (Fig. 2). The smart contact element will provide information like contact pressures, plastic strains, temperatures, but also damage variables and yield stresses in the vicinity of the surface. All these information will be sent to the Library of Damage Indicators, which is an external database based on experimental and numerical data. It includes critical values on contact conditions (contact pressure, plastic strain, sliding velocity, temperature, roughness and etc.), with respect to materials, and lubricants. The basic idea is to fill the L.D.I. with as much information as possible, obtained from industrial forming processes and/or laboratory testing. Input data will be related to the physical, chemical, thermo-mechanical conditions of contact. Output data (i.e. surface roughness, surface defect deposition, lubricant film breakdown) will be the type and the range of wear (adhesive, abrasive, surface damage) that may occur on tool surface.

3.1. Numerical modelling

In order to gather more insight on the plastic deformation of specimens tested on the UST, a finite element analysis connected to each experimental test has been performed. Experimental results were used to calibrate the numerical simulations.

The UST was simulated with the commercial finite element program ABAQUS Version 6.12. The specimen was modelled as a deformable 2D solid body subject to plane strain with nominal dimensions given in Section 2.3 while the fixed stand and the contactor were modelled as rigid elements. The specimen was discretized in implicit elements CPE4R: the element size of 0.1 mm was determined via convergence analysis. The Coulomb’s friction law was used to model friction. The coefficient of friction involved for each computation was identified from the experimental UST results according to [12].

The parameters of the stress-strain curve were fitted using a mathematical power curve $\sigma=K\times\varepsilon^n$ MPa as indicated in the E646 ASTM International Standard [14], and then inserted in ABAQUS with K=498 and n=0.101.

3.2. Statistical setup of plastic deformation

In the present study, 22 experimental tests (USTs) were performed with plastic strain in the vicinity of the contact zone ranging from 0.006 to 0.112. In order to ease the use of the experimental results, Sturges' rule was used to define "classes" of plastic strain [15]. The number of classes is given by:

$$k = 1 + 3.332Log(N), \text{ where } N = 22 \text{ (tests)} \quad (1)$$

First, the range of plastic deformation Ep experienced by the specimen for different values of the imposed penetration depth is determined by:

$$E_p = \varepsilon_{\max} - \varepsilon_{\min} \quad (2)$$

where ε_{max} is 0.112 (i.e. a maximum of plastic deformation generated at the interface between contactor/specimen using a penetration depth Δh = 180µm); ε_{min} is 0.006 (i.e. a maximum plastic deformation generated at the interface between contactor/specimen using a penetration depth of Δh = 40µm). The size of each grade can then be obtained from the relationship:

$$L = E_p / k \quad (3)$$

By setting classes and their corresponding upper and lower limits defined on the basis of Eqs. (1-3), it is possible to determine the mean values and corresponding standard deviations summarized in Table 1.

Table 1. Classes of plastic strains corresponding to different penetration depths.

Grade	Ep1	Ep2	Ep3	Ep4	Ep5	No Lubr.
Plastic strain range	0.006-0.027	0.027-0.048	0.048-0.069	0.069-0.09	0.09-0.112	
Plastic strain mean value	0.014	0.035	0.052	0.073	0.107	0.518

4. Settlement of the Library of Damage Indicators.

4.1. Quantification of material transfer onto the contactor

3D-Optical profilometer inspections revealed that contactor and workpiece roughness changes in magnitude and distribution because of forming. By analysing these differences it is possible to make hypotheses on the mechanisms behind the modifications that occur during sliding progress. Those changes are the result of local plastic deformation, combined with the increase of local temperature. They involve the transfer of aluminium alloy to the tool surface, into the so called galling evolution. The topography of tool and specimen surfaces that were submitted to cold forging are shown in Fig. 3. Green arrows in Fig. 3 indicate the direction of sliding.

The thickness of the local layer of workpiece material transferred to the tool was evaluated by inspecting the tool surface before and after the forming sequence. For that purpose, the maximum ten-point height Rz (the difference between the averages of the 5 highest and 5 lowest points on the surface) was computed.

The differences between the final and initial contour of profile thickness correspond to the thickness of the layer of aluminium material transferred from the specimen to the contactor. In Fig. 4 is quantified the amount of material transferred onto the contactor surface as a function of the range of plastic strain. It appears that the thickness of the transfer layer increases with plastic deformation. The amount of material deposited onto the tool surface may not be significant at low plastic strain, as for the deformation classes Ep1 to Ep4 (see Fig. 4).

4.2. Evolution of friction

Fig. 5 plot the values of friction coefficient with respect to the level of plastic strain. The figure shows friction coefficient average values and corresponding standard deviations evaluated at each level of plastic strain. By introducing the MoS2 lubricant in the UST it is possible to reduce the value of friction coefficient from 0.5-0.7 (values determined from the two non-lubricated UST.) to 0.006-0.15.

The Coulomb's friction coefficient does not change much as long as the plastic strain remains in the Ep1 to Ep4 grade range, and is related to the thickness value of material transfer (max. 5 µm). This behaviour may occur

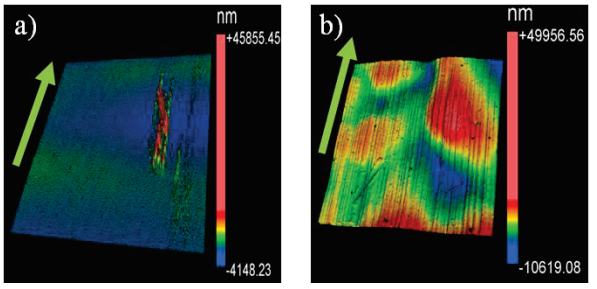

Fig 3. Distribution of surface roughness after forging: a) contactor zone I; b) specimen.

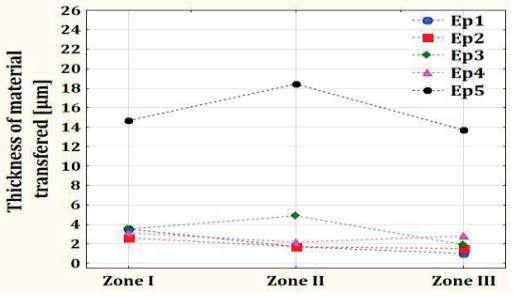

Fig. 4. Variation of thickness of the material layer deposited on the tool surface in the UST, longitudinal (i.e. sliding) direction.

because the galling deposition is fully immersed in the layer of MoS_2 lubricant (since the thickness of the lubricant is 10µm) during UST. As expected, the friction coefficient strongly increases as deformation grade evolves from Ep4 to Ep5, consequence to the major level of thickness of material transfer measured for domain Ep5 (i.e. around 20 µm) while breaking of lubricant film occurs.Insignificant fluctuations in friction coefficient values may derive from having imposed different process parameters, small variations of temperature, roughness discrepancies, or solid lubricant inhomogeneity. However, differences in friction coefficient values were not found to be statistically significant.

In addition, optical inspection of contact surfaces provides necessary information to evaluate quantitatively and qualitatively the surface defect transfer. This approach allows to precisely measure any modification of the interacting surfaces.

Fig. 5 presents the connection between the class of plastic strain and the surface defects. For the low plastic strain (i.e. Ep1) a transfer layer appears on the contactor surface as a single mark extended along the sliding direction. The numbers of longitudinal marks increase with the plastic strain (Ep2- Ep4) and finally the overall contactor surfaces is covered by transferred workpiece material due to lubricant breakdown for the Ep5 experience.

5. Validation of new expert system approach

The flat strip drawing test has been chosen to quantify the Tool Surface Degradation Expert System ability to predict tool degradations. Flat strip drawing tests were performed using a contactor shape as specified in [16], characterized by a wedge semi-angles of 10.5° and a face length of 4.84 mm. Finite element computations of the FSDT were run to calculate the effective plastic strain near the contact zone at the tool/strip interface. Finite element computations lead to an estimation of the plastic strain equal to 0.115, which corresponds to class Ep5 of the L.D.I. So, according to the Expert System, a strong adhesion of aluminium material on tool surface is expected (Fig. 5).

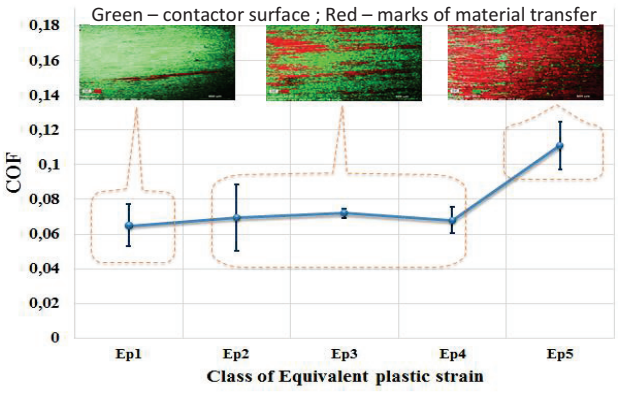

Fig. 5. Variation of friction coefficient and adhesion as a function of plastic deformation during the UST.

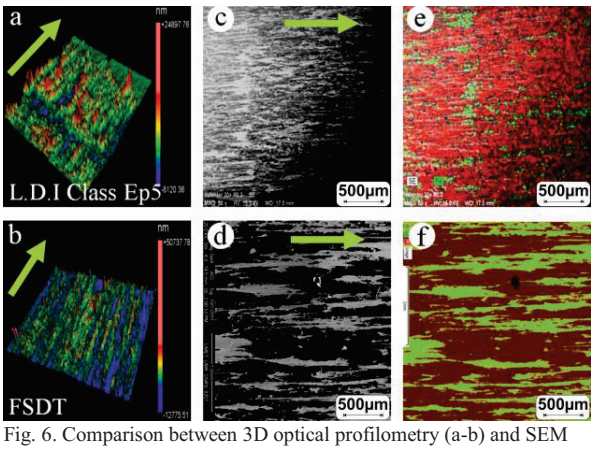

Fig. 6. Comparison between 3D optical profilometry (a-b) and SEM (c-d). SEM-EDS (e-f). Red=aluminium, green=iron.

Flat strip drawing tests have been performed on three aluminium strips. The aluminium alloy is the same as the one used to feed the Library of Damage Indicators, and strips are lubricated with MoS_2. Flat strip drawing tool roughness has been measured and SEM observations have been performed.

Comparison of flat strip drawing tool defects with the defect recorded in the Library of Damage Indicators and coming from the Upsetting-Sliding Test are in good accordance (Fig. 6). When the values of plastic deformation applied for both tests are in the same class, the surface topography on both tools emphasize the same characteristics of surface profile defect: the thickness of material transfer is equal and the surface area covered by the transfer layer is in the same range (even if the flat strip drawing tool presents a more stripy surface, the total part of the tool covered with aluminium is the same as the UST tool). This result confirms the validity of the first stage of the Tool Surface Degradation Expert System approach.

6. Conclusion.

In this research, an innovative approach is proposed to predict the risk of tool damage by linking results of finite element computations to a specific database, called Library of Damage Indicators. In the present work, which corresponds to the very first stage of the development of the database, only the plastic strain at the vicinity of contactor/specimen interface is taken into account. The first result allows estimating the quantity of tool degradation occurring during a flat strip drawing test just by performing a finite element computation.

Acknowledgements

The authors gratefully acknowledge the support of the International Campus on Safety and Intermodality in Transportation (www.cisit.org), the Nord-Pas-de-Calais Region, the European Community, the Ministry of Higher Education and Research, and the French National Center for Scientific Research.

References

[1] P.M.G.P. Moreira, A.M.P. de Jesus, A.S. Ribeiro, P.M.S.T. de Castro, 2008. Fatigue crack growth in friction stir welds of 6082-T6 and 6061-T6 aluminium alloys: A comparison. Theoretical and Applied Fracture Mechanics 50, 81–91.
[2] H. Yoshimura, K. Tanaka, 2000. Precision forging of aluminum and steel. Journal of Materials Processing Technology 98, 196-204.
[3] T.M. Almeida Bugio, R.F. Martins, L.L. das Neves, 2013. Failure analysis of fuel tanks of a lightweight ship. Engineering Failure Analysis, 272-285.
[4] N. Hägele, C.M. Sonsino, 2011. Structural durability design recommendations for forged automotive aluminium chassis components submitted to spectrum and environmental loadings by the example of a tension strut. Procedia Engineering 10, 330–339.
[5] W.R.D. Wilson, S. Sheu, 1988. Real area of contact and boundary friction in metal forming. International Journal of Mechanical Sciences, 30, 7, 475-489.
[6] T.A. Stolarski,1990, A probabilistic approach to wear prediction. J. Phys. D: Appl. Phys., 24, 1143–1149.
[7] A. Fischer, K. Bobzin, 2009, Friction, Wear and Wear Protection. s.l. : WILEY-VCH Verlag GmbH & Co. KGaA, Weinheim, 84.
[8] P. Groche, N. Moeller, H. Hoffmann, J. Suh, 2011. Influence of gliding speed and contact pressure on the wear of forming tools. Wear 271, 2570– 2578.
[9] K. Ersoy-Nurnberg,G. Nurnberg, M. Golle, H. Hoffmann, 2008. Simulation of wear on sheet metal forming tools—An energy approach. Wear, 265, 11–12, 1801–1807.
[10] J.F. Archard, 1953. Contact and rubbing of flat surfaces. Journal of Applied Physics. 24, 981–988.
[11] Z. Semaria, A. Aid, A. Benhamena, A. Amrouche, M. Benguediab, A. Sadok, N. Benseddiq, 2013. Effect of residual stresses induced by cold expansion on the crack growth in 6082 aluminum alloy. Engineering Fracture Mechanics, 99, 159–168.
[12] L. Lazzarotto, L. Dubar, A. Dubois, P. Ravassard, J. Oudin, 1997. Identification of Coulomb's friction coefficient in real contact conditions applied to a wire drawing process. Wear 211, 54-63.
[13] L Dubar, A Dubois, M Dubar, 2006. Friction and wear phenomena in cold metal forming: an integrated approach, Proceedings of the Institution of Mechanical Engineers, Part B: Journal of Engineering Manufacture, 220, 1, 1-10.
[14] Materials, ASTM E646-00 Standard Test Method for Tensile Strain-Hardening Exponents (n-Values) of Metallic Sheet.
[15] D.W. Scott, 2011. Sturges' and Scott's Rules. International Encyclopedia of Statistical Science. ISBN: 3642048978, 1563-1566.
[16] M.P.F. Sutcliffe, H.R. Lea, D. Farrugia, 2003. Simulation of transfer layer formation in strip drawing of stainless steel. Wear 254, 523-531.